https://doi.org/10.17221/189/2023-CJFS

Optimised formulation and characterisation of oregano essential oil edible composite films by response surface methodology

*Hekun Duan[1], Zitian Yuan[1], Suyan Liu[1], Liang Jin[2], Ping Wen[3], Yaqi Wang[4], Fuhao Hu[1], Fei Han[1]**

[1]*Department of Pharmacy, Jiangxi University of Chinese Medicine, Nanchang, China*
[2]*Institute of Biological Resources, Jiangxi Academy of Sciences, Nanchang, China*
[3]*Institute of Chinese Medicine, Jiangxi Provincial Institute of Traditional Chinese Medicine, Nanchang, China*
[4]*Key Laboratory of Modern Traditional Chinese Medicine Preparations, Ministry of Education, Jiangxi University of Chinese Medicine, Nanchang, China*

**Corresponding author: hanfei8454871@163.com*

Citation: Duan H., Yuan Z., Liu S., Jin L., Wen P., Wang Y., Hu F., Han F. (2024): Optimised formulation and characterisation of oregano essential oil edible composite films by response surface methodology. Czech J. Food Sci., 42: 31–44.

Abstract: The objective of this research is to prepare a composite packaging film by integrating oregano essential oil (OEO) into a chitosan (CS)/polyvinyl alcohol (PVA) matrix to enhance the preservative properties of food packaging films. For this purpose, the study established multiple quality evaluation methods for composite films. The composite weights for each evaluation indicator were calculated through the analytic hierarchy process-coefficient of variation (AHP-CV), deriving the comprehensive score value (OD). Employing OD as the ultimate evaluation indicator, the optimal preparation formula for the OEO composite film was ascertained by applying response surface methodology (RSM), incorporating insights gained from single-factor experiments. The results showed that the optimum formulation was CS 1.51 g, PVA 3.51 g, glycerin 1.97 g, and Tween-80 0.51 g. The OD for the OEO composite film prepared under these conditions was 83.95 ± 0.12%, closely matching the predicted value of 83.91%. Characterisation further confirmed the cross-linking action between CS and PVA, while the inclusion of OEO enhanced the antimicrobial activity of the composite film. These findings suggest incorporating OEO into composite packaging films holds considerable potential for enhancing food packaging applications.

Keywords: antimicrobial properties; food packaging film; chitosan; polyvinyl alcohol

As the public becomes increasingly aware of the risks and hazards associated with using synthetic additives and preservatives in the food industry, there is a growing emphasis on the efficacy of natural antimicrobials for food preservation (El-Saber Batiha et al. 2021). The food industry aims to reduce synthet-

Supported by the National Natural Science Foundation of China (Project No. 81560659), by the Natural Science Foundation of Jiangxi Province, China (Project No. 20232BAB206169), by the Science and Technology Research Project of Education Department of Jiangxi Province, China (Project No. GJJ2200903), and with the Graduate Innovation Project of Jiangxi Province, China (Project No. YC2023-S765).

https://doi.org/10.17221/189/2023-CJFS

ic preservative use due to highlighted concerns about accumulation and long-term toxicity in toxicological studies (Sambu et al. 2022; Yang et al. 2023). Natural plant essential oils provide a significant and safe alternative for retarding the deterioration and oxidation of food during storage (Bukvicki et al. 2023). Therefore, exploring the potential of essential oils as alternatives to traditional synthetic fungicides for preserving fruits and vegetables is of paramount scientific significance (Shi et al. 2021). Nevertheless, despite the promising potential of essential oils as alternatives to chemical preservatives, specific limitations must be tackled before contemplating their application in food systems (Fernández-López and Viuda-Martos 2018).

Oregano essential oil (OEO) is a volatile plant essential oil renowned for its antimicrobial and antioxidant effects (Wu et al. 2022). The antimicrobial action of OEO is attributed to its ability to target the cell walls and membranes of bacteria, resulting in significant damage to both the cell walls and membranes. This damage leads to the formation of cytoplasmic vacuoles and stainless vesicles, causing disruption and interruption of intracellular structures (Lu et al. 2018). The OEO also induces an imbalance in intracellular osmotic pressure, ultimately leading to cell necrosis. Furthermore, carvacrol is the main component of OEO, which induces changes in the bacterial cell surface, affecting the initial adhesion during biofilm development and further inhibiting bacterial growth (Tapia-Rodriguez et al. 2017). The OEO has demonstrated remarkable antimicrobial effectiveness against common foodborne pathogens, establishing itself as a natural antimicrobial agent for food preservation. The study evaluated the antimicrobial activity of *Staphylococcus aureus*, a common foodborne pathogen isolated from poultry meat, confirming that all isolated strains were sensitive to the OEO (Marques et al. 2015). Another study determined the antimicrobial activity of the OEO against six foodborne pathogens, including three Gram-negative bacteria (*Escherichia coli*, *Salmonella enterica*, and *Vibrio cholerae*) and three Gram-positive bacteria (*S. aureus*, *Listeria monocytogenes*, and *Bacillus cereus*) (Evangelista-Barreto et al. 2018). The OEO exhibited food-grade antimicrobial activity against these foodborne Gram-negative and Gram-positive pathogens, making it a natural preservative for preventing spoilage bacteria in food.

The OEO has received approval from the United States. Food and Drug Administration (FDA) as a food additive, affirming its safety and preservation attributes (Veenstra and Johnson 2019; Zhan et al. 2022). Even though the OEO has these advantages, it also has certain limitations. The main constraints of using OEO as a food additive are its high volatility, low solubility, intense irritability, and the potential to negatively impact the sensory characteristics of food (Li et al. 2020). Recent attention has shifted toward incorporating various active substances, including natural antimicrobial agents like essential oils, into food packaging materials, effectively enhancing performance, inhibiting microbial growth in food, and improving preservation quality (Punia Bangar et al. 2021). Incorporating ginger essential oil into agarose-sodium alginate double-layer films enhances their barrier properties and water sensitivity while imparting excellent antimicrobial activity (Zhang et al. 2023). Adding tea tree essential oil to starch/furcellaran/gelatin films reduces the thermal stability of the films, with a significant improvement in antioxidant performance (Jamróz et al. 2018). Including clove essential oil in alginate/κ-carrageenan-based edible films reduces the mechanical properties of the films, enhances flexibility, and effectively improves antioxidant and antimicrobial properties (Prasetyaningrum et al. 2021). Most research reports emphasise that adding essential oil to composite films affects various properties of the films and enhances their antioxidant capability and antimicrobial activity. Therefore, the development of food packaging films enriched with OEO presents a significant avenue to enhance the antimicrobial efficacy of the packaging material.

Polymeric food packaging films represent some of the most widely utilised materials in safeguarding food against microbial threats, boasting characteristics such as flexibility, strength, stiffness, and impermeability to both oxygen and moisture (Huang et al. 2019). Chitosan (CS), a natural linear polymer, stands out due to its biocompatibility, non-toxicity, and remarkable film-forming capability (Shariatinia 2019). Polyvinyl alcohol (PVA) is a synthetic polymer material suitable for combining with other polymers to improve physical, thermal, and barrier properties (Wahyuningsih et al. 2016). Currently, composite films combining CS and PVA polymers have garnered significant attention in food packaging due to their excellent mechanical and physical properties, along with good thermal stability (Narasagoudr et al. 2020; Nwabor et al. 2020; Terzioğlu et al. 2021). Research has unveiled the compatibility of PVA and CS polymers, developing novel

https://doi.org/10.17221/189/2023-CJFS

composites with superior attributes (Choo et al. 2016). Interestingly, the acetylated groups of PVA chains can be ionised and negatively charged, and the phenolic hydroxyl groups of carvacrol can act as Lewis electron acceptors, which can facilitate the binding of PVA to the phenolic hydroxyl groups of carvacrol and thus to binding to the polymer chains to form Lewis adducts (Tampau et al. 2020). This specific interaction of PVA with the phenolic hydroxyl groups of carvacrol better loads OEO onto CS/PVA packaging materials, which reduces the volatility of oregano oil and improves its stability.

This study aimed to develop an edible composite film incorporating OEO to enhance the antimicrobial activity of food preservation packaging. Five evaluation indicators for the composite film were examined, and the analytic hierarchy process-coefficient of variation (AHP-CV) method was employed to compute composite weights for each evaluation criterion, facilitating the determination of a comprehensive score (OD). Using response surface methodology (RSM), the optimal formulation of the OEO composite film was determined, and its chemical and antimicrobial properties were evaluated.

MATERIAL AND METHODS

Material

Chitosan (biological reagent) was purchased from Sinopharm Chemical Reagent, China. Alcohol (17-88 grade) was obtained from McLean Biochemical Technology, China. Tween-80 was sourced from Tianjin Fuchen Chemical Reagent Factory, China. Analytically pure glacial acetic acid, glycerin, 95% ethanol and anhydrous ethanol were purchased from Xilong Science, China. Oregano oil and carvacrol were purchased from Jiangxi Xinsen Natural Vegetable Oil, China.

Film preparation

Reference to the preparation method of CS film, with slight modifications (Siripatrawan and Harte 2010). A film-forming solution was prepared by dissolving a specific amount of CS into a 1% acetic acid solution. An appropriate quantity of PVA was added to the solution, and the mixture was heated to 85 °C in a water bath for 20 min. Glycerin was incorporated into the film-forming solution as a plasticiser. After an additional 20 min, Tween-80 was added to the solution. Once the temperature descended below 60 °C, OEO was introduced and homogenised at 10 000 rpm for 2 min using a laboratory digital display high-speed dispersing homogeniser (FJ300-SH; Huxi, China). Subsequently, 10 mL of the OEO film-forming solution was poured onto a clean glass plate with dimensions of 15 × 5 cm. The glass plate was oscillated to ensure uniform distribution of the film-forming solution, and the film was dried at 60 °C for 80 min. Following drying, the film was meticulously cut into the appropriate specifications and set aside for later use.

Determination of quality evaluation of OEO composite film

Formability. The formability of the composite films underwent evaluation using five indicators: film-forming property, colour uniformity, smoothness, bubble, and flexibility. The assessment followed the scoring criteria documented in Table 1. The maximum attainable score was set at 100 points, with each evaluation indicator allocated a potential 20 points. After evaluating the composite films, the total scores for each composite film were calculated.

Melting time. The melting time of the composite film is defined as the duration between the film's immersion and its complete dissolution. In this study, we employed this parameter to assess the safety of the composite film. Initially, a 1 000 mL beaker was filled with distilled water at 37.5 °C. The prepared OEO film was trimmed to dimensions of 3 × 3 cm, with both ends firmly secured using two clamps to maintain a consistent width of 3 cm between them. The upper part of one clamp was affixed with a specialised tool, suspending it at the centre of the beaker's mouth. The other clamp was employed to simulate a controlled force. Under

Table 1. Grading criteria

Evaluation	Film-forming property	Colour uniformity	Smoothness	Bubble	Flexibility
Excellent	16~20	16~20	16~20	16~20	16~20
Good	11~15	11~15	11~15	11~15	11~15
General	6~10	6~10	6~10	6~10	6~10
Poor	0~5	0~5	0~5	0~5	0~5

https://doi.org/10.17221/189/2023-CJFS

experimental conditions, both clamps ensured the film remained perpendicular to the water's surface, solely influenced by gravity, and fully immersed in the liquid. The timer started when the film was wholly immersed, and the time taken for the film to dissolve entirely in distilled water was recorded.

Tensile strength. The thickness of the film plays a crucial role in determining the mechanical properties in terms of the film's tensile strength. The film thickness was measured by digital micrometre (DM025; As one, China) with an accuracy of 0.001 mm. Tensile strength measurements were conducted using an electronic stripping testing machine (BLD-200N; Labthink, China). The prepared film was cut into dimensions of 5 × 3 cm, with both ends securely affixed to the machine, maintaining a width of 3 cm. The parameters of the electronic stripping testing machine were adjusted to achieve a tensile rate of 100 mm·min^{-1}. The test was initiated and continued until the film reached its breaking point, at which the reading, representing the tensile strength of the composite film, was recorded.

Adhesion. The prepared composite film was cut into 3 × 3 cm dimensions and attached to the 8 mm high test platform of the physical property analyser (TVT-6700; Potong Ruihua, China), dripped with 10 mL of distilled water. Subsequently, the cylindrical probe N672035 (Wilmad, USA) with a diameter of 35 mm was moistened with 3 mL of distilled water and used to conduct the adhesive force test on the film. The test parameters were set as follows: pre-test speed of 5.0 mm·s^{-1}, test speed of 3 mm·s^{-1}, post-test upward speed of 10 mm·s^{-1}, compression distance of 15 mm, pressure at 1 000 Pa, trigger force at 50 mN, two cycles, and a residence time of 0 s. The adhesive force of the film was quantified as the resistance encountered when the cylindrical probe was pressed and lifted.

Content. Carvacrol, recognised as the principal constituent of OEO, serves as a critical evaluation indicator for OEO (Ju et al. 2019). The quantification of carvacrol content in the OEO film was accomplished through ultraviolet spectrophotometry. The film was cut into 2 × 2 cm dimensions and positioned within a 10 mL beaker. Subsequently, 2.5 mL of distilled water was introduced into the beaker, thoroughly stirred, and then transferred to a 50 mL volumetric flask. Absolute ethyl alcohol was incrementally added to the volumetric flask, reaching the desired scale, after which the volume was fixed, and the contents were thoroughly mixed. The resulting filtrate was employed as the test sample. Based on the ultraviolet absorption spectrum of carvacrol in the supplementary data [see Electronic Supplementary Material (ESM), Figures S1–S2, Tables S1–S4], λ = 276 nm was chosen as the measuring wavelength for the experiment. A standard curve for the carvacrol solution was constructed, and the linear regression equation for this standard curve was provided in the ESM. Employing 95% (*v*/*v*) ethanol as the blank control, the absorbance at λ = 276 nm was determined, allowing the calculation of carvacrol content using the linear regression equation.

Determination of weight and score of each indicator

Analytic hierarchy process (AHP). The AHP is a subjective weighting method employed to assess the relative importance of two indicators based on subjective judgments (Wang et al. 2018). Through establishing a judgment matrix, the weight of each indicator can be determined. In this study, we developed an AHP structure model and utilised the 1–9 scale method to evaluate the relative importance of the five indicators (Table 2) (Ishizaka and Labib 2011). The weight coefficient results obtained through AHP are presented in Table 3.

Coefficient of variation (CV). The CV serves as an objective means to assess the outcomes of experiments. It operates on the fundamental principle that higher measured indicators within the evaluation system signify a more substantial distinction among the

Table 2. Analytic hierarchy process grading criteria of each hierarchy

Scale	Definition of importance
9	extremely important
7	strongly important
5	obviously important
3	slightly important
1	equally important
2, 4, 6, 8	an intermediate score between adjacent importance
Reciprocal	if the importance of Party *A* to Party *B* is *a*, the importance of Party *B* to Party *A* is 1/*a*

https://doi.org/10.17221/189/2023-CJFS

Table 3. Priority matrix and weight coefficients for evaluating five indicators

Indicators	Content	Melting time	Tensile strength	Adhesion	Exterior	Weight coefficient (%)
Content	1	2	4	5	7	42.82
Melting time	1/2	1	3	5	6	29.43
Tensile strength	1/4	1/3	1	3	4	14.23
Adhesion	1/5	1/5	1/3	1	5	9.53
Exterior	1/7	1/6	1/4	1/5	1	4.00

objects under evaluation (Liu et al. 2018a). The CV was calculated by Equation 1.

$$V_i = \frac{\sigma_i}{x_i}\left(i = 1, 2, ..., n\right) \quad (1)$$

where: V_i – CV for the i^{th}, σ_i – standard deviation for the i^{th}; x_i – mean for the i^{th}.

The equation for calculating weight can be expressed as follows:

$$W_i = \frac{V_i}{\sum_{i=1}^{n} V_i} \quad (2)$$

where: W_i – weight of the CV.

The weight coefficients for content, melting time, tensile strength, adhesion, and exterior calculated using the CV method described above are as follows: 14.95, 7.67, 28.65, 46.47, and 2.26%, respectively.

Calculation of composite weights

The weights of the five composite indicators are calculated by combining the two methods of AHP and CV. The calculation method can be expressed as follows:

$$W_c = \frac{W_i \times W_A}{\sum_{i=1}^{n} W_i \times W_A} \quad (3)$$

where: W_c – composite weight; W_i – weight of CV; W_A – weight of AHP; the composite weights of content (W_{c_1}), melting time (W_{c_2}), tensile strength (W_{c_3}), adhesion (W_{c_4}), and exterior (W_{c_5}) were 37.10, 13.09, 23.63, 25.66, and 0.52%, respectively.

Comprehensive score

OD values are used to evaluate the overall level of multiple evaluation indicators. The *OD* was calculated by Equation 4:

$$OD = \left(\frac{W_{c_1} R_1}{R_{1_{max}}} + \frac{W_{c_2} R_2}{R_{2_{max}}} + \ldots + \frac{W_{c_n} R_n}{R_{n_{max}}}\right) \times 100\ \% \quad (4)$$

where: *OD* – comprehensive score; W_{c_n} – composite weight value calculated by each group; R_n – response value measured by each group; $R_{n_{max}}$ – maximum measured value.

Characterisation of films

Fourier transform infrared (FTIR). The chemical structure of films was conducted using the FTIR Spectrometer (Spectrum2; PerkinElmer, USA). The samples were processed by the KBr-pellet method, and the infrared spectral curves were collected at a step of 4 cm^{-1} in a period of 400 to 4 000 cm^{-1} wavenumbers.

Differential scanning calorimetry (DSC). The thermal stability of the samples was examined using a differential scanning calorimeter (Diamond DSC 4000; PerkinElmer, USA). Under a nitrogen atmosphere, the samples were heated at 10 °C per minute from 30 to 400 °C.

Antimicrobial assay. Before commencing antimicrobial assessments, suspensions for each strain were meticulously prepared. Detailed information on all strains is presented in Table 4. The colonies of *S. aureus*, *E. coli*, *S. dysenteriae*, *P. aeruginosa*, and *K. pneumoniae* were inoculated into a liquid Luria-Bertani (L-B) agar plate. At the same time, *Candida albicans* were cultivated in liquid yeast extract peptone dextrose (YPD) agar plate. The strains of 50 μL were evenly coated on the surface of the corresponding agar plate. Subsequently, all agar plates were transferred to an incubator and incubated for 24 h at 37 °C. Following this incubation period, 100 μL of bacterial solution from each agar plate was aseptically inoculated onto fresh agar plates and cultured in the incubator for 24 h. Individual bacterial colonies were meticulously collected using sterile inoculating rings and subsequently cultured in a suitable broth medium within the incubator for an additional 24 h to yield bacterial suspensions for subsequent experimentation.

https://doi.org/10.17221/189/2023-CJFS

Table 4. Information of strains

Strains	Medium	Strain number
Staphylococcus aureus	L-B agar plate	ATCC25923
Escherichia coli	L-B agar plate	CMCC44103
Shigella dysenteriae	L-B agar plate	CMCQ(B)51105
Pseudomonas aeruginosa	L-B agar plate	ATCC27853
Klebsiella pneumoniae	L-B agar plate	CMCC(B)46117
Candida albicans	YPD agar plate	ATCC10231

L-B – Luria-Bertani; YPD – yeast extract peptone dextrose

The antimicrobial efficacy of the OEO composite film against tested strains was assessed using the disc diffusion method (Azócar et al. 2012). Initially, different volumes of OEO were incorporated into the composite films: a low volume (1 mL), a medium volume (3 mL), and a high volume (5 mL). A blank film-forming solution devoid of OEO was employed as the control. Then, 50 μL of bacterial suspension was taken from the broth medium of each strain and evenly coated on an L-B agar plate and a YPD agar plate with a coating rod. The OEO composite films, prepared in various amounts as described earlier, were precisely cut into 6 mm diameter circles using a hole punch. These OEO films were attached to the surface of the agar plate using tweezers and incubated at 37 °C for 24 h. Following the incubation period, we evaluated the antibacterial activity of the composite films by measuring the diameter of the clear zone (expressed in mm) surrounding each film.

Statistical analysis. Design Expert software (version 13.0) was used to design the RSM experiments. The graph was plotted with the aid of Origin (version 2021). Analysis of variance (ANOVA) was performed using SPSS software (version 26.0.) Prescription validation and antimicrobial experiments were repeated three times, and the results were expressed as 'mean ± standard deviation' (mean ± SD).

RESULTS AND DISCUSSION

Single-factor experiments

Using *OD* as the final evaluation indicator, we explored the impact of the amount of PVA, CS, glycerin, and Tween-80 on various indicators of OEO composite films (Figure 1). PVA amounts were tested in the 1–6 g range, showing an increasing trend in *OD*. Adhesion peaked at 4 g, crucial for food packaging films, leading to its selection for the subsequent single-factor experiment. For CS, amounts varied from 0.5 to 3 g, with *OD* peaking at 0.5 g, but film-forming quality and efficiency were suboptimal. Thus, 2 g of CS was chosen for the subsequent single-factor experiment. Glycerin amounts (1–6 g) were explored, with *OD* reaching its maximum at 2 g, prompting its selection for the subsequent single-factor experiment. The impact Tween-80 on *OD* was assessed with varying amounts (1–6 g). In comparison, 4 g showed the maximum effect, potential toxicity beyond 3 g, and adverse effects on film appearance at higher amounts. This led to the selection of 1 g as the central level for subsequent RSM experiments.

Response surface analysis

The Box-Behnken design was used to optimise the formulation. The composite weights of the five indicators were calculated, and the *OD* (*Y*) of the OEO composite film served as the final response value. The Box-Behnken response surface design comprised four factors, each with three levels (Table 5). The second-order regression equation is as follows:

$$\begin{aligned} Y = {} & 73.12 + 2.52A - 4.38B - 0.690C + \\ & - 2.69D + 4.94AB - 4.79AC + 6.37AD + \\ & - 7.53BC + 4.36BD - 3.45CD - 3.00A^2 + \\ & - 1.52B^2 - 0.8086C^2 - 3.64D^2 \end{aligned} \quad (5)$$

where: Y – *OD*; A, B, C, and D – the coded values of the chosen factors.

The experimental results of RSM are shown in Table 6. The results indicated that the model was highly significant ($P < 0.01$), and the lack of fit for the model was not statistically significant ($P > 0.05$) (Table 7). Among the four factors affecting the preparation formula of OEO film, factors *A* and *D* and the interaction terms *AB*, *AC*, and *BD* significantly impacted the *OD* ($P < 0.05$). Factor *B* and the interaction terms AD and BC significantly influenced *OD* ($P < 0.01$).

https://doi.org/10.17221/189/2023-CJFS

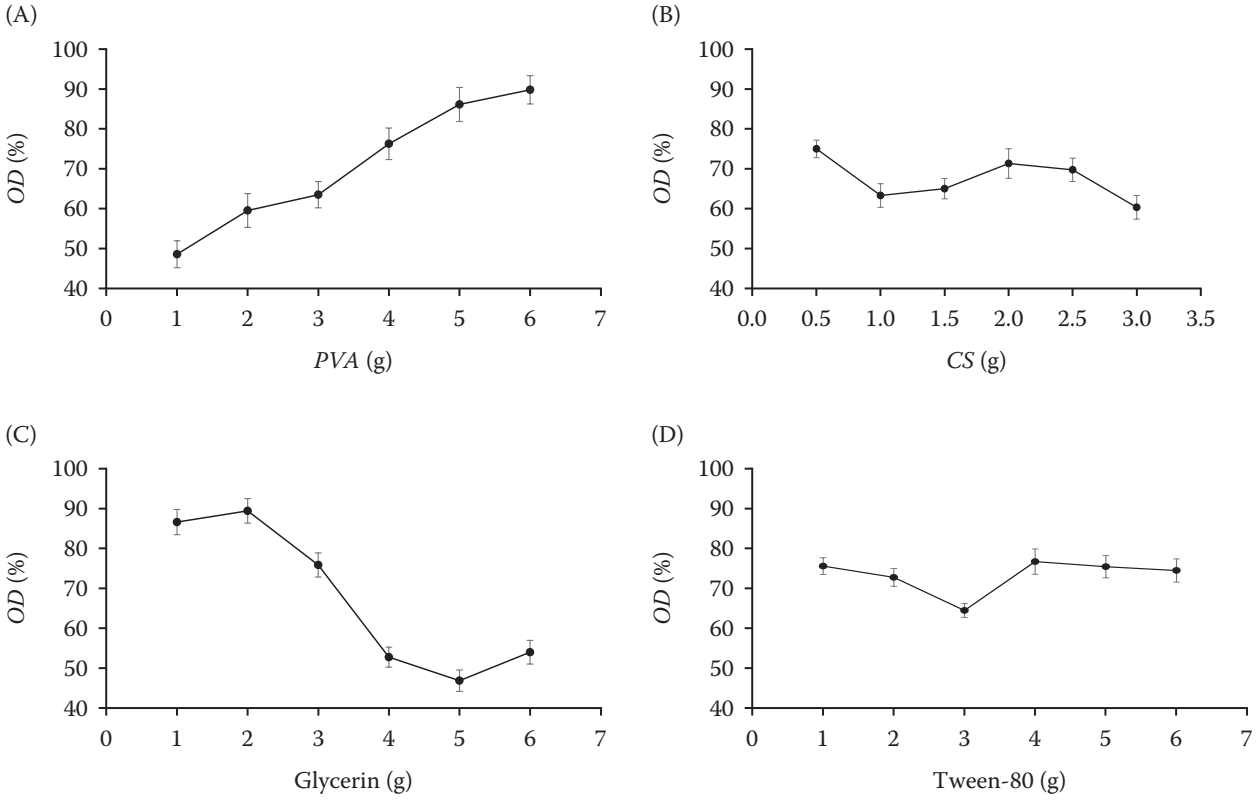

Figure 1. Effect of different amounts on the *OD* of composite film (A) PVA, (B) CS, (C) glycerin, and (D) Tween-80

OD – comprehensive score; PVA – polyvinyl alcohol; CS – chitosan

The fitting statistics showed that the difference between the corrected coefficient R^2 and the prediction coefficient R^2 was less than 0.2, indicating their reasonability and consistency. Therefore, regression determination coefficients in Equation 5 were R^2 = 0.8706, adjusted R^2 = 0.7411, and predicted R^2 = 0.5642, signifying that the regression equation fits well with the actual experiments and could be employed to determine the optimal preparation prescription.

The response surface diagrams were generated to illustrate relationships between independent and dependent variables (Figure 2). The optimum formulation for the OEO composite film preparation was determined: PVA 3.51 g, CS 1.51 g, glycerin 1.97 g, and Tween-80 0.51 g. Under these optimised conditions, the predicted *OD* of the OEO composite film was calculated at 83.91%. We conducted triplicate experiments based on the optimum formulation to validate the model's accuracy, comparing the experimental results with the model's predictions. The experimental *OD* values were found to be 83.95 ± 0.12%. Notably, the experimental *OD* closely aligned with the predicted value of 83.91%, underscoring the reliability of our obtained model and the accuracy of its predictive outcomes.

Characterisation analysis

FTIR. FTIR is an imperative tool to characterise and determine the chemical structure and molecular in-

Table 5. Factors and levels

Level	*A*	*B*	*C*	*D*
	PVA (g)	CS (g)	glycerin (g)	Tween-80 (g)
–1	3.50	1.50	1.50	0.50
0	4.00	2.00	2.00	1.00
1	4.50	2.50	2.50	1.50

PVA – polyvinyl alcohol; CS – chitosan

https://doi.org/10.17221/189/2023-CJFS

Table 6. The result of the response surface methodology

Run	*A*	*B*	*C*	*D*	*OD* (%)
	PVA (g)	CS (g)	glycerin (g)	Tween-80 (g)	
1	4.00	2.00	2.50	1.50	62.48
2	3.50	2.00	2.00	0.50	75.55
3	4.50	2.00	2.50	1.00	67.09
4	4.00	2.00	1.50	1.50	68.72
5	4.00	1.50	1.50	1.00	69.51
6	4.00	2.00	2.00	1.00	70.31
7	3.50	2.00	1.50	1.00	60.93
8	4.00	2.00	1.50	0.50	68.13
9	4.00	2.00	2.00	1.00	81.51
10	4.00	1.50	2.50	1.00	83.65
11	4.50	2.00	2.00	0.50	64.68
12	3.50	2.00	2.50	1.00	66.63
13	4.00	2.00	2.50	0.50	75.68
14	4.00	1.50	2.00	0.50	78.75
15	4.50	1.50	2.00	1.00	67.90
16	4.00	2.00	2.00	1.00	73.64
17	3.50	1.50	2.00	1.00	74.58
18	4.00	2.00	2.00	1.00	68.24
19	4.50	2.00	1.50	1.00	80.53
20	3.50	2.50	2.00	1.00	59.59
21	4.00	2.50	2.00	1.50	64.85
22	4.00	2.00	2.00	1.00	71.89
23	4.00	2.50	2.50	1.00	57.86
24	4.00	2.50	2.00	0.50	59.55
25	4.50	2.50	2.00	1.00	72.67
26	4.50	2.00	2.00	1.50	71.02
27	4.00	1.50	2.00	1.50	66.59
28	4.00	2.50	1.50	1.00	73.86
29	3.50	2.00	2.00	1.50	56.40

PVA – polyvinyl alcohol; CS – chitosan; *OD* – comprehensive score

teractions of composite blends (Istiqomah et al. 2022). Figure 3 shows the FTIR spectra of CS, OEO/CS, CS/PVA, and OEO/CS/PVA. The FTIR spectrum of pure CS showed the characteristic broad absorption peak at 3 370 cm^{-1}, attributed to the presence of -OH and -NH_2 groups within the polymer chain. A weaker absorption band at 2 889 cm^{-1} corresponded to stretching vibrations of C-H in alkane groups. The 1 692, 1 583, and 1 373 cm^{-1} peaks were ascribed to the amide I, II, and -CH_2 bending variation, respectively. The bands observed from 1 070 to 1 157 cm^{-1} correspond to peaks indicative of the stretching vibrations of C-O bonds, characteristic of the saccharide structure (Liu et al. 2018b; Zheng et al. 2019). While observing the FTIR spectra of the OEO/CS, it was noted that aside from the characteristic absorption peak of CS, there was an additional absorption peak at 1 206 cm^{-1}, corresponding to the phenolic hydroxyl group in the primary constituent of OEO (carvacrol). Absorption peaks observed at 1 385 and 1 370 cm^{-1} were attributed to the vibrational modes of the two methyl groups within the isopropyl moiety of the carvacrol molecule. Furthermore, it was observed that the characteristic

https://doi.org/10.17221/189/2023-CJFS

Table 7. Analysis of variance

Source	Sum of squares	*df*	Mean square	*F*-value	*P*-value
Model	1 225.60	14	87.54	6.72	0.0005**
A	75.95	1	75.95	5.83	0.0300*
B	230.36	1	230.36	17.69	0.0009**
C	5.75	1	5.75	0.44	0.5171
D	86.87	1	86.87	6.67	0.0217*
AB	97.67	1	97.67	7.50	0.0160*
AC	91.60	1	91.60	7.04	0.0189*
AD	162.53	1	162.53	12.48	0.0033**
BC	227.11	1	227.11	17.45	0.0009**
BD	76.17	1	76.17	5.85	0.0298*
CD	47.54	1	47.54	3.65	0.0767
A^2	58.20	1	58.20	4.47	0.0529
B^2	15.03	1	15.03	1.15	0.3008
C^2	4.23	1	4.23	0.33	0.5776
D^2	86.08	1	86.08	6.61	0.0222*
Residual	182.26	14	13.02	–	–
Lack of fit	78.32	10	7.83	0.30	0.9436
Pure error	103.94	4	25.98	–	–
Corrected total	1 407.86	28	–	–	–

*,** Significant at 0.05 and 0.01 level, respectively; *df* – degree of freedom

absorption peak of CS is absent in the range from 1 070 to 1 157 cm^{-1} when compared to spectrum *A*. This phenomenon could be attributed to the interaction of vibrational modes and hybridisation effects. The combination of OEO and CS may result in the formation of new vibrational modes or alterations in the intensity and position of pre-existing vibrational modes, leading to the blurring of the peak at this location. In the CS/PVA film spectrum, the C-O stretching vibrations of CS at 1 070 cm^{-1} shifted to lower wavenumbers. The absorption peak at this position also indicates the presence of glycerin. Additionally, the -OH stretching vibrations of CS at 3 370 cm^{-1} shifted to 3 308 cm^{-1}, indicating the occurrence of intermolecular interactions between CS and PVA molecules. These lower wave shifts implied increased interchain hydrogen bonding between the CS carbonyl and PVA hydroxyl groups (Wu et al. 2018). When comparing the spectrum of CS/PVA film to that of the CS/PVA film containing OEO, it was observed that the FTIR spectra of OEO/CS/PVA film did not exhibit any new peaks, and the characteristic absorption peaks of both films were nearly identical. In general, the addition of OEO does not impact the chemical structure of the PVA/CS film, confirming the excellent compatibility between OEO and the CS/PVA composite film.

DSC. The DSC curves obtained for CS, OEO, CS/PVA, and OEO/CS/PVA are shown in Figure 4. CS exhibited an endothermic region within the 90 to 100 °C range and a distinct exothermic peak between 300 and 350 °C, likely attributed to oxidation or cross-linking reactions generating new compounds during heat treatment. In the DSC curve of OEO, notably sharp heat absorption peaks were evident at 59 and 232 °C, signifying two phase transitions and associated heat absorption. From the DSC curves of CS/PVA and OEO/CS/PVA, it can be observed that the characteristic absorption peaks and exothermic peaks of CS and OEO are primarily absent, indicating that a cross-linking reaction has occurred between CS and PVA, resulting in the formation of new compounds. When OEO is incorporated into the CS/PVA film, the absorption peak slightly shifts towards lower temperatures, which may be related to the thermal degradation of the film matrix (Lin et al. 2020). However, the transition temperature width of CS/PVA films is closely aligned

https://doi.org/10.17221/189/2023-CJFS

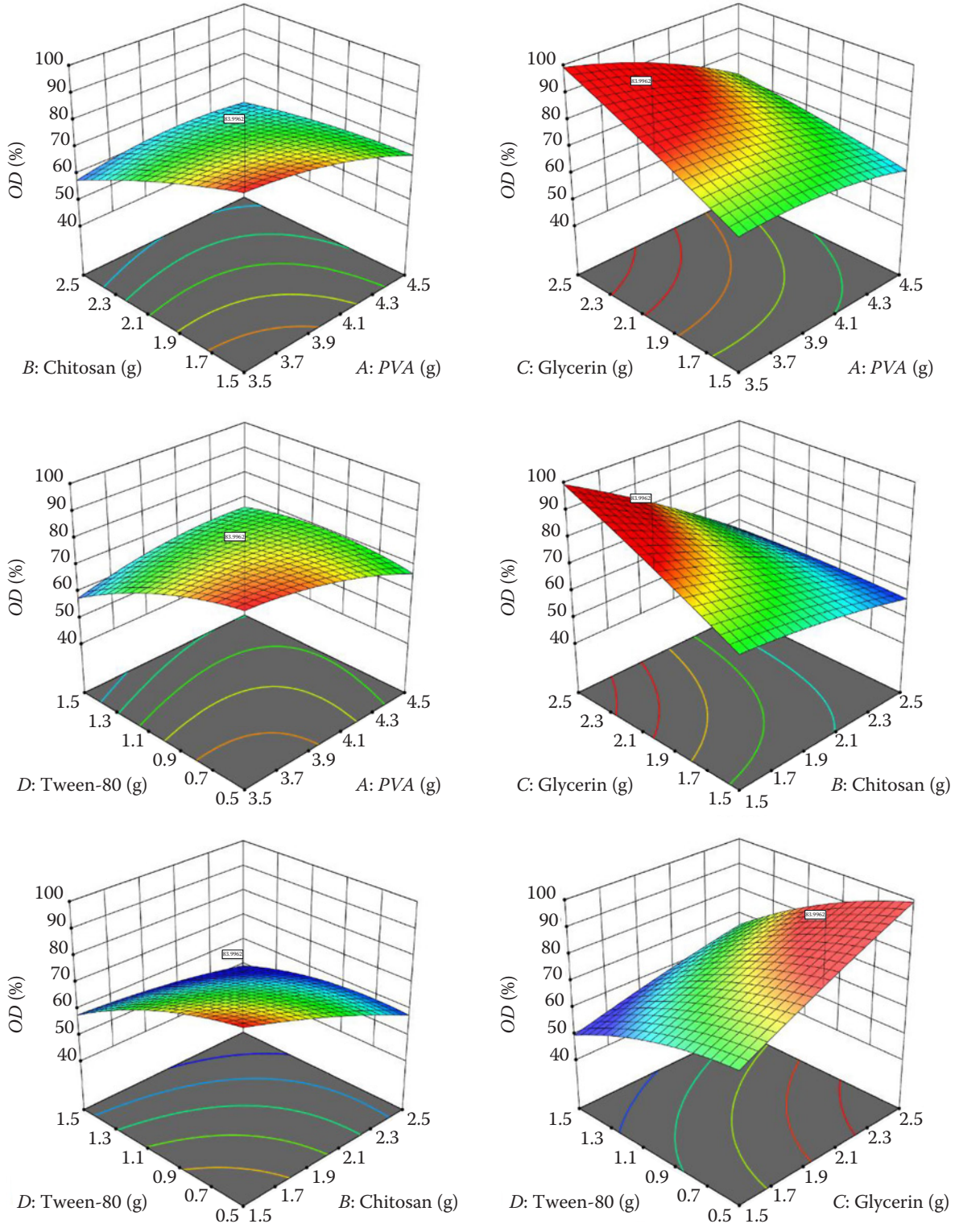

Figure 2. Response surface plots showing the interaction of various factors on *OD*

PVA – polyvinyl alcohol; *OD* – comprehensive score

with that of the OEO composite films. The addition of OEO does not significantly affect the exothermic and endothermic properties of the film during heating, indicating no apparent physical or thermodynamic phase changes, thereby confirming the high compatibility between CS/PVA and OEO.

https://doi.org/10.17221/189/2023-CJFS

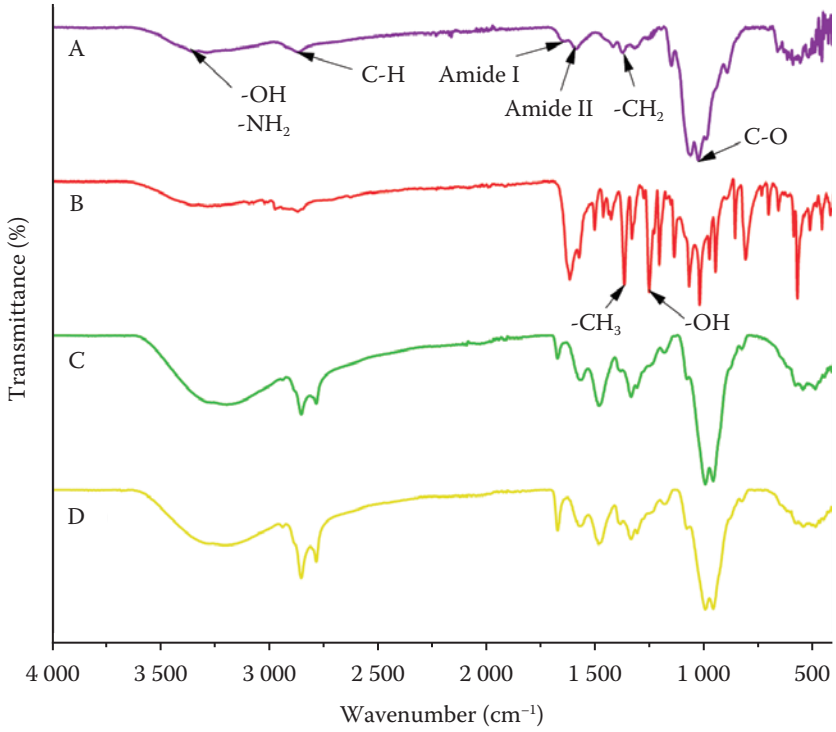

Figure 3. Fourier transform infrared spectra

A – CS; B – OEO/CS; C – CS/PVA; D – OEO/CS/PVA;
CS – chitosan; OEO – oregano essential oil; PVA – polyvinyl alcohol

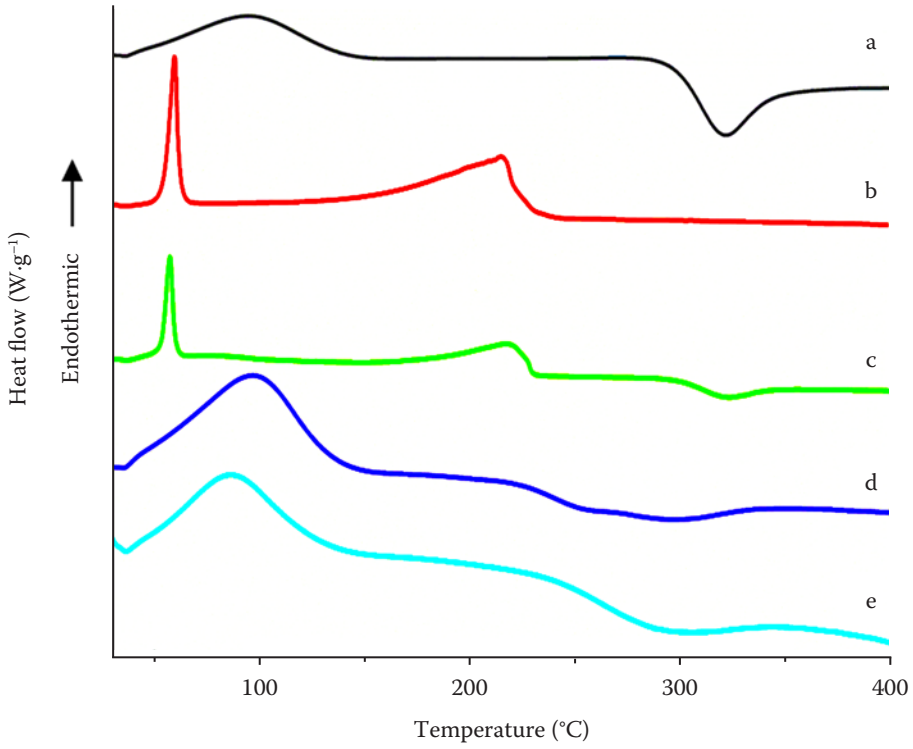

Figure 4. Differential scanning calorimetry curve

a – CS; b – OEO; c – OEO/CS; d – CS/PVA; e – OEO/CS/PVA;
CS – chitosan; OEO – oregano essential oil; PVA – polyvinyl alcohol

https://doi.org/10.17221/189/2023-CJFS

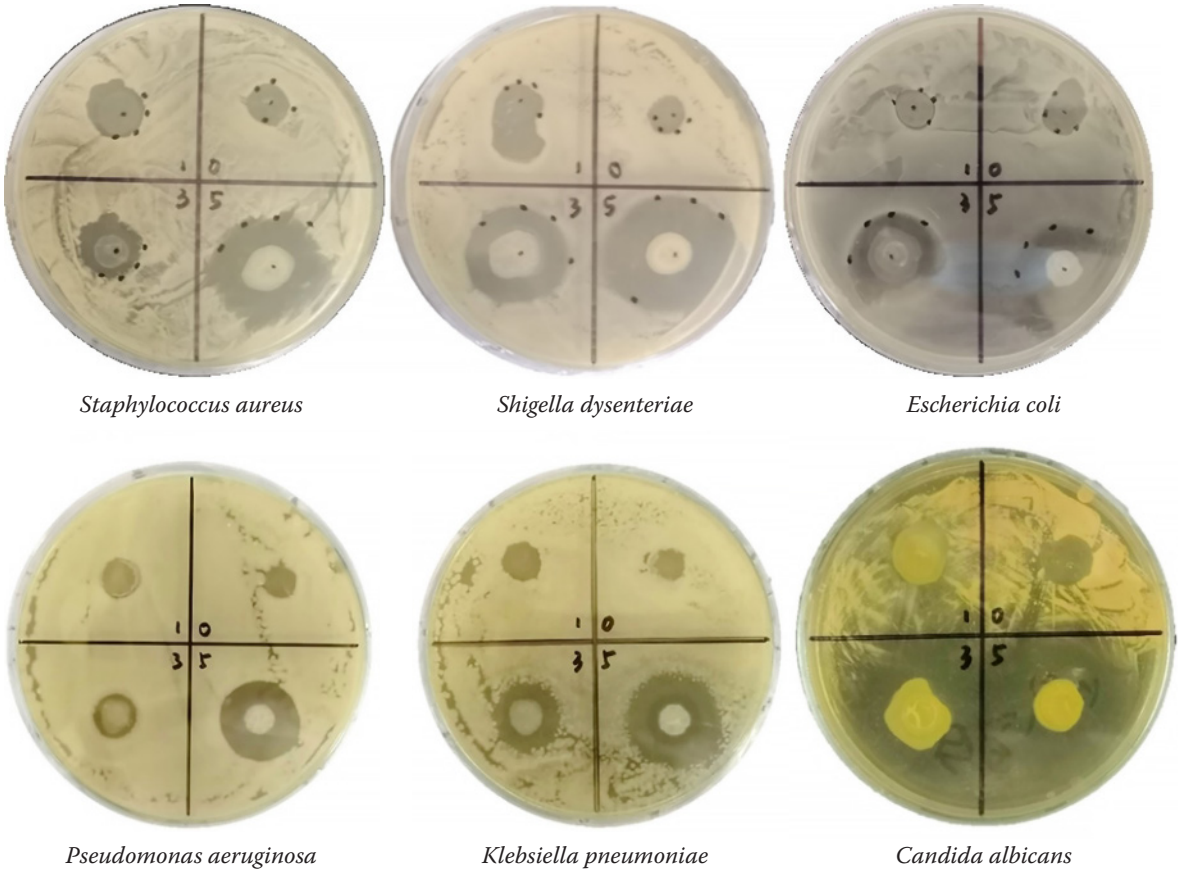

Figure 5. Inhibition zone of oregano essential oil composite films on 6 kinds of bacteria

Antimicrobial properties. It could be seen from Figure 5 that the composite films supported on a disk created a zone of inhibition in bacterial growth, implying that both the blank composite films and the composite films containing OEO exhibited antimicrobial activity. The blank composite films had lower antimicrobial properties, which could be attributed to the electrostatic interaction between the positively charged CS and the negatively charged microbial cell membranes, thus exerting the antimicrobial effect (Ke et al. 2021). The results of antimicrobial experiments indicated that the OEO composite film had a significant inhibitory effect on all the tested foodborne pathogens, and with the increase in OEO content, the OEO composite film strengthened the inhibition of six strains (Table 8). In summary, the addition of OEO expanded the range of antimicrobial zones, which confirmed that OEO improved the antimicrobial properties of the composite packaging films.

Table 8. Inhibition zone diameter measured

Strains	Inhibition zone diameter – OEO film (mm)			
	0 mL	1 mL	3 mL	5 mL
Staphylococcus aureus	9.11 ± 0.38^{a}	11.33 ± 0.66^{b}	16.89 ± 0.38^{c}	23.78 ± 0.39^{d}
Shigella dysenteriae	8.89 ± 0.38^{a}	11.11 ± 0.38^{b}	18.45 ± 0.39^{c}	23.78 ± 0.77^{d}
Escherichia coli	9.11 ± 0.77^{a}	9.78 ± 0.77^{a}	19.33 ± 0.67^{c}	23.55 ± 0.39^{d}
Pseudomonas aeruginosa	8.00 ± 0.00^{a}	9.78 ± 0.77^{b}	12.00 ± 0.00^{c}	16.89 ± 1.02^{d}
Klebsiella pneumoniae	9.11 ± 0.38^{a}	10.44 ± 0.77^{a}	17.11 ± 1.02^{c}	26.22 ± 1.39^{d}
Candida albicans	9.11 ± 1.02^{a}	11.55 ± 0.39^{b}	34.67 ± 0.67^{c}	37.11 ± 0.77^{d}

$^{a–d}$ Different letters within the same row are statistically significant ($P < 0.05$); OEO – oregano essential oil

https://doi.org/10.17221/189/2023-CJFS

CONCLUSION

This study successfully prepared an edible composite film incorporating OEO into CS/PVA, enhancing the antimicrobial performance of food packaging films. Through the RSM, the optimal formulation for the OEO edible film was determined: 1.51 g CS, 3.51 g PVA, 1.97 g glycerin, and 0.51 g Tween-80. The *OD* of the composite film prepared under the optimised conditions was 83.95 ± 0.12%, close to the predicted value (83.91%). The results showed that CS and PVA exhibited favourable compatibility, and incorporating OEO into the CS/PVA film enhanced its antimicrobial activity. In conclusion, the present work reflects that the OEO edible film is a promising packaging material with excellent potential as a food preservative product.

REFERENCES

Azócar I., Vargas E., Duran N., Arrieta A., González E., Pavez J., Kogan M.J., Zagal J.H., Paez M.A. (2012): Preparation and antibacterial properties of hybrid-zirconia films with silver nanoparticles. Materials Chemistry and Physics, 137: 396–403.

Bukvicki D., D Alessandro M., Rossi S., Siroli L., Gottardi D., Braschi G., Patrignani F., Lanciotti R. (2023): Essential oils and their combination with lactic acid bacteria and bacteriocins to improve the safety and shelf life of foods: A review. Foods, 12: 3288.

Choo K., Ching Y., Chuah C., Julai S., Liou N. (2016): Preparation and characterization of polyvinyl alcohol-chitosan composite films reinforced with cellulose nanofiber. Materials, 9: 644.

El-Saber Batiha G., Hussein D.E., Algammal A.M. (2021): Application of natural antimicrobials in food preservation: Recent views. Food Control, 126: 108066.

Evangelista-Barreto N.S., Costa Júnior P.S.P., Vieira B.B. (2018): Control of psychrotrophic bacteria and *Escherichia coli* in frescal type fish sausage using oregano essential oil (Controle de bacterias psicrotróficas e *Escherichia coli* em linguiça de peixe tipo frescal adicionada de óleo essencial de orégano). Boletim Do Instituto De Pesca, 44: 68–73. (in Spanish)

Fernández-López J., Viuda-Martos M. (2018): Introduction to the special issue: Application of essential oils in food systems. Foods, 7: 56.

Huang T., Qian Y., Wei J., Zhou C. (2019): Polymeric antimicrobial food packaging and its applications. Polymers, 11: 560.

Ishizaka A., Labib A. (2011): Review of the main developments in the analytic hierarchy process. Expert Systems with Applications, 38: 14336–14345.

Istiqomah A., Utami M.R., Firdaus M., Suryanti V., Kusumaningsih T. (2022): Antibacterial chitosan – *Dioscorea alata* starch film enriched with essential oils optimally prepared by following response surface methodology. Food Bioscience, 46: 101603.

Jamróz E., Juszczak L., Kucharek M. (2018): Development of starch-furcellaran-gelatin films containing tea tree essential oil. Journal of Applied Polymer Science, 135: 46754.

Ju J., Xie Y., Guo Y., Cheng Y., Qian H., Yao W. (2019): The inhibitory effect of plant essential oils on foodborne pathogenic bacteria in food. Critical Reviews in Food Science and Nutrition, 59: 3281–3292.

Ke C., Deng F., Chuang C., Lin C. (2021): Antimicrobial actions and applications of chitosan. Polymers, 13: 904.

Li L., Song W., Shen C., Dong Q., Wang Y., Zuo S. (2020): Active packaging film containing oregano essential oil microcapsules and their application for strawberry preservation. Journal of Food Processing and Preservation, 44: e14799.

Lin D., Wu Z., Huang Y. (2020): Physical, mechanical, structural and antibacterial properties of polyvinyl alcohol/oregano oil/graphene oxide composite films. Journal of Polymers and the Environment, 28: 638–646.

Liu W., Li Q., Zhao J. (2018a): Application on floor water inrush evaluation based on AHP variation coefficient method with GIS. Geotechnical and Geological Engineering, 36: 2799–2808.

Liu Y., Wang S., Lan W. (2018b): Fabrication of antibacterial chitosan-PVA blended film using electrospray technique for food packaging applications. International Journal of Biological Macromolecules, 107: 848–854.

Lu M., Dai T., Murray C.K., Wu M.X. (2018): Bactericidal property of oregano oil against multidrug-resistant clinical isolates. Frontiers in Microbiology, 9: 2329.

Marques J.D.L., Volcão L.M., Funck G.D., Kroning I.S., Da Silva W.P., Fiorentini Â.M., Ribeiro G.A. (2015): Antimicrobial activity of essential oils of *Origanum vulgare* L. and *Origanum majorana* L. against *Staphylococcus aureus* isolated from poultry meat. Industrial Crops and Products, 77: 444–450.

Narasagoudr S.S., Hegde V.G., Chougale R.B., Masti S.P., Dixit S. (2020): Influence of boswellic acid on multifunctional properties of chitosan/poly (vinyl alcohol) films for active food packaging. International Journal of Biological Macromolecules, 154: 48–61.

Nwabor O.F., Singh S., Paosen S., Vongkamjan K., Voravuthikunchai S.P. (2020): Enhancement of food shelf life with polyvinyl alcohol-chitosan nanocomposite films from bioactive eucalyptus leaf extracts. Food Bioscience, 36: 100609.

Prasetyaningrum A., Utomo D.P., Raemas A.F.A., Kusworo T.D., Jos B., Djaeni M. (2021): Alginate/κ-carrageenan-based edible films incorporated with clove essential oil:

https://doi.org/10.17221/189/2023-CJFS

Physico-chemical characterization and antioxidant-antimicrobial activity. Polymers, 13: 354.

Punia Bangar S., Chaudhary V., Thakur N., Kajla P., Kumar M., Trif M. (2021): Natural antimicrobials as additives for edible food packaging applications: A review. Foods, 10: 2282.

Sambu S., Hemaram U., Murugan R., Alsofi A.A. (2022): Toxicological and teratogenic effect of various food additives: An updated review. Biomed Research International, 2022: 1–11.

Shariatinia Z. (2019): Pharmaceutical applications of chitosan. Advances in Colloid and Interface Science, 263: 131–194.

Shi Z., Jiang Y., Sun Y., Min D., Li F., Li X., Zhang X. (2021): Nanocapsules of oregano essential oil preparation and characterization and its fungistasis on apricot fruit during shelf life. Journal of Food Processing and Preservation, 45: e15649.

Siripatrawan U., Harte B.R. (2010): Physical properties and antioxidant activity of an active film from chitosan incorporated with green tea extract. Food Hydrocolloids, 24: 770–775.

Tampau A., González-Martínez C., Chiralt A. (2020): Polyvinyl alcohol-based materials encapsulating carvacrol obtained by solvent casting and electrospinning. Reactive and Functional Polymers, 153: 104603.

Tapia-Rodriguez M.R., Hernandez-Mendoza A., Gonzalez-Aguilar G.A., Martinez-Tellez M.A., Martins C.M., Ayala-Zavala J.F. (2017): Carvacrol as potential quorum sensing inhibitor of *Pseudomonas aeruginosa* and biofilm production on stainless steel surfaces. Food Control, 75: 255–261.

Terzioğlu P., Güney F., Parın F.N., Şen İ., Tuna S. (2021): Biowaste orange peel incorporated chitosan/polyvinyl alcohol composite films for food packaging applications. Food Packaging and Shelf Life, 30: 100742.

Veenstra J.P., Johnson J.J. (2019): Oregano (*Origanium vulgare*) extract for food preservation and improving gastrointestinal health. International Journal of Nutrition, 3: 43–52.

Wahyuningsih K., Iriani E.S., Fahma F. (2016): Utilization of cellulose from pineapple leaf fibers as nanofiller in polyvinyl alcohol-based film. Indonesian Journal of Chemistry, 6: 181–189.

Wang H., Chen Z., Feng X., Di X., Liu D., Zhao J., Sui X. (2018): Research on network security situation assessment and quantification method based on analytic hierarchy process. Wireless Personal Communications, 102: 1401–1420.

Wu Y., Ying Y., Liu Y., Zhang H., Huang J. (2018): Preparation of chitosan/poly vinyl alcohol films and their inhibition of biofilm formation against *Pseudomonas aeruginosa* PAO1. International Journal of Biological Macromolecules, 118: 2131–2137.

Wu T., Yang F., Jiao T., Zhao S. (2022): Effects of dietary oregano essential oil on cecal microorganisms and muscle fatty acids of luhua chickens. Animals, 12: 3215.

Yang J., Goksen G., Zhang W. (2023): Rosemary essential oil: Chemical and biological properties, with emphasis on its delivery systems for food preservation. Food Control, 154: 110003.

Zhan X., Tan Y., Lv Y., Fang J., Zhou Y., Gao X., Zhu H., Shi C. (2022): The antimicrobial and antibiofilm activity of oregano essential oil against *Enterococcus faecalis* and its application in chicken breast. Foods, 11: 2296.

Zhang B., Liu Y., Peng H., Lin Y., Cai K. (2023): Effects of ginger essential oil on physicochemical and structural properties of agar-sodium alginate bilayer film and its application to beef refrigeration. Meat Science, 198: 109051.

Zheng K., Xiao S., Li W., Wang W., Chen H., Yang F., Qin C. (2019): Chitosan-acorn starch-eugenol edible film: Physico-chemical, barrier, antimicrobial, antioxidant and structural properties. International Journal of Biological Macromolecules, 135: 344–352.

Received: November 16, 2023
Accepted: January 26, 2024
Published online: February 16, 2024